Enhanced Proportional-Resonant Current Controller for Unbalanced Stand-alone DFIG-based Wind Turbines

Van-Tung Phan* and Hong-Hee Lee†

Abstract - An enhanced control strategy for variable-speed unbalanced stand-alone doubly-fed induction generator-based wind energy conversion systems is proposed in this paper. The control scheme is applied to the rotor-side converter to eliminate stator voltage imbalance. The proposed current controller is developed based on the proportional-resonant regulator, which is implemented in the stator stationary reference frame. The resonant controller is tuned at the stator synchronous frequency to achieve zero steady-state errors in rotor currents without decomposing the positive and negative sequence components. The computational complexity of the proposed control algorithm is greatly simplified, and control performance is significantly improved. Finally, simulations and experimental results are presented to verify the feasibility and the robustness of the proposed control scheme.

Keywords: Doubly fed induction generator (DFIG), Resonant controller, Unbalanced load, Stand-alone wind system

1. Introduction

In recent years, many variable-speed wind turbines for both grid-connected and stand-alone wind power generation systems have been intensively developed based on a doubly-fed induction generator (DFIG) [1]-[4], which offers several advantages compared with other generator systems. The advantages include ease of speed control, decoupled active and reactive power capability, and reduced rate of inverter up to approximately 20%-30% of total system power.

Majority of DFIG studies have focused on symmetrical network voltage or balance connected loads. However, for practical cases, unexpected conditions exist, including network disturbances, unbalanced grid voltages, and unbalanced load conditions. For DFIG systems, if the voltage imbalance condition is not taken into account by the control system, the stator voltage could become highly unbalanced. Such a scenario creates heat on the stator windings and reduces the lifetime of the generator.

The control and operation of a grid-connected DFIG system under an unbalanced grid voltage has been widely investigated in the literature [5]-[8]. To eliminate torque pulsation due to the presence of negative sequence current, one control method based on a rotor-side converter (RSC) has been outlined in [5]. In the study, the torque pulsation at twice the supply frequency has been reduced by generating the required compensating rotor currents. In [6], a detailed investigation of the impact of an unbalanced stator voltage on the pulsations of DFIG stator and rotor currents, torque, and stator active and reactive power has been presented. The proposed control method has also been performed on an RSC controller with an inadequate capability for reducing both torque and active power oscillations. To overcome this problem, the coordinated control for both the rotor-side and grid-side converters within a DFIG was proposed in [7]-[8]. Based on this improvement, dynamic performance of DFIG systems can be significantly improved.

Apart from taking into account a grid-connected DFIG system, the control and operation of a stand-alone or isolated DFIG-based wind energy system (Fig. 1) have been presented in [2]. For stand-alone DFIG applications, the system itself must regulate both the output voltage and the frequency in a stable manner. One proposed compensation method is briefly introduced in [9], in which a stand-alone DFIG supplying an unbalanced load is considered. However, in [9], no detailed explanation on the design of the current controller or the unbalanced voltage compensation method has been shown to exist. In another paper by the same authors [10], modeling and controlling of a DFIG based on a grid-side converter (GSC) for unbalanced operation

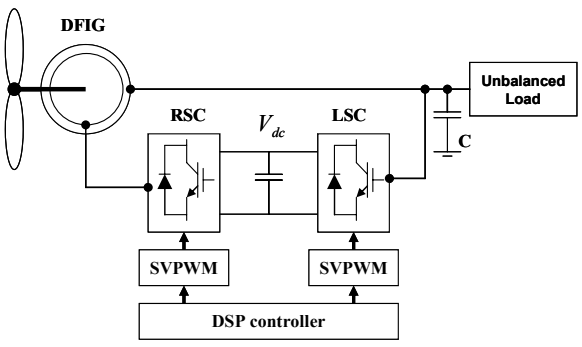

Fig. 1. Typical configuration of a stand-alone DFIG-based wind generator feeding to unbalanced loads.

† Corresponding Author: School of Electrical Engineering, University of Ulsan, Korea. (hhlee@mail.ulsan.ac.kr)
* School of Electrical and Electronic Engineering, University of Ulsan, Korea. (tungvp@yahoo.com)
Received: January 16, 2010; Accepted: June 11, 2010

have been investigated for both grid-connected and stand-alone applications. In [9] and [10], dual synchronous rotating reference frames, called positive and negative rotating reference frames, have been used for decomposing the positive and negative sequence components of the current values. The main drawback of this approach is the considerable time delay due to complicated calculations, such as multiple frame transformations and decompositions that, in turn, led to errors with respect to the command values. Furthermore, a control scheme for a current controller requires a wide bandwidth to make it suitable for controlling the separate sequences.

Among previously proposed current control strategies, proportional-integral (PI) controllers have been widely used in current controllers to compensate errors because of their simplicity and effectiveness. The PI controller has certain limitations and drawbacks in regulating accurately the AC reference currents due to the limited bandwidth. To remove these shortcomings, a resonant controller has been introduced in [11] and [12] as an improved solution in terms of the AC reference tracking performance in grid-connected converters. Due to the infinite gain at a selected resonant frequency, this controller is capable of completely eliminating the steady-state control error at the said frequency.

In this paper, a new control strategy using the PR controller for variable-speed unbalanced stand-alone DFIG systems is proposed to enhance the compensation capability and improve dynamic performance. The proposed PR current controller was constructed in the stator stationary reference frame instead of the dual frames used in [6]-[8]. The resonant regulator was tuned at the synchronous stator frequency. As a result, the proposed current controller can directly regulate both positive and negative sequence components without the need for sequential decomposition of the measured rotor currents, as shown in [9]-[10]. The complexity in calculations of the proposed control algorithm was greatly simplified and the control performance was significantly improved. The proposed control method was investigated solely with respect to the RSC of a DFIG control system to compensate the generated stator voltage imbalances caused by the unbalanced loads. In addition, simulations and experimental setup were implemented under different unbalanced load conditions to verify the feasibility and robustness of the compensation method with the proposed control scheme.

2. The Proposed Control Scheme

The control and operation of balanced stand-alone DFIG systems are described in [2]. In this section, an analysis is performed on a vector-controlled DFIG-based variable-speed wind energy system, which supplies electrical energy to an unbalanced stand-alone load or an isolated grid. Under this load condition, the stator voltage, current, torque, flux, and power include both positive and negative sequence components that cause fluctuations in the synchronous frequency in the stator stationary reference frame. The following subsection will describe the control strategy implemented in the RSC to compensate for unbalanced stator voltages. A method of calculating the reference rotor currents for the proposed current controllers is also outlined.

2.1 Control of an Unbalanced DFIG

The main purpose of the RSC is to control the stator voltage magnitude and frequency. In stand-alone operations, a DFIG-based wind energy system has to supply constant voltage and frequency to the stator terminals, regardless of variations in the rotor speed. In this work, the control system for a DFIG under an unbalanced load was developed based on a stator flux-oriented vector control strategy. Fig. 2 shows a vector diagram, which represents the relationship between a stator stationary frame ($\alpha_s\beta_s$), a rotor frame ($\alpha_r\beta_r$) rotating with an angular speed (ω_r), a positive frame (dq^+), rotating with an angular speed (ω_s), and a negative frame (dq^-) rotating with an angular speed ($-\omega_s$). The superscripts "+" and "-" represent positive and negative synchronous reference frames, respectively. The vector F denotes the value of the voltage, current, or flux in the stator's flux-oriented reference frame.

Under an unbalanced load condition, the most convenient method to analyze the DFIG model is to use a positive reference frame rotating at a speed of ω_s and a negative reference frame rotating at a speed of $-\omega_s$. According to Fig. 2, the relationship of a vector F between different frames is illustrated as follows:

$$\begin{aligned} F_{\alpha_s\beta_s} &= F_{dq}^{+} e^{j\omega_s t} = F_{dq}^{-} e^{-j\omega_s t} \\ F_{dq}^{+} &= F_{dq}^{-} e^{-j2\omega_s t} \end{aligned} \tag{1}$$

The stator and rotor current, voltage, and flux vectors F can be expressed in the stator's stationary reference frame with their respective positive and negative sequences as:

$$F_{\alpha_s\beta_s} = F_{\alpha_s\beta_s+} + F_{\alpha_s\beta_s-} = F_{dq+}^{+} e^{j\omega_s t} + F_{dq-}^{-} e^{-j\omega_s t}, \tag{2}$$

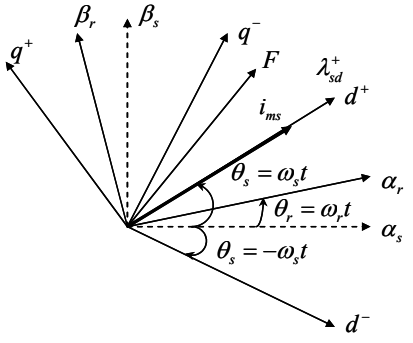

Fig. 2. Vector diagram representing the relationship between different reference frames.

where the subscripts + and - represent the positive and negative sequence components, respectively.

According to (2), the quantities in the stator's stationary reference frame are the sum of the ac components with the frequencies of $\pm\omega_s$. The control target is developed based on the stationary reference frame. Therefore, the dynamic DFIG equations are described as follows:

$$v_{s\alpha\beta}^{s} = R_s i_{s\alpha\beta}^{s} + \frac{d\lambda_{s\alpha\beta}^{s}}{dt}, \tag{3}$$

$$v_{r\alpha\beta}^{s} = R_r i_{r\alpha\beta}^{s} + \frac{d\lambda_{r\alpha\beta}^{s}}{dt} - j\omega_r \lambda_{r\alpha\beta}^{s}, \tag{4}$$

$$\lambda_{s\alpha\beta}^{s} = L_s i_{s\alpha\beta}^{s} + L_m i_{r\alpha\beta}^{s}, \text{ and} \tag{5}$$

$$\lambda_{r\alpha\beta}^{s} = L_r i_{r\alpha\beta}^{s} + L_m i_{s\alpha\beta}^{s}. \tag{6}$$

From (3)-(6), the rotor voltages in the stationary reference frame can be expressed as:

$$v_{r\alpha}^{s} = R_r i_{r\alpha}^{s} + \sigma L_r \frac{di_{r\alpha}^{s}}{dt} + \frac{L_m}{L_s}\left(v_{s\alpha}^{s} - R_s i_{s\alpha}^{s}\right) + \omega_r \left(L_r i_{r\beta}^{s} + L_m i_{s\beta}^{s}\right) \tag{7}$$

and

$$v_{r\beta}^{s} = R_r i_{r\beta}^{s} + \sigma L_r \frac{di_{r\beta}^{s}}{dt} + \frac{L_m}{L_s}\left(v_{s\beta}^{s} - R_s i_{s\beta}^{s}\right) - \omega_r \left(L_r i_{r\alpha}^{s} + L_m i_{s\alpha}^{s}\right), \tag{8}$$

where R_s is the stator resistance, L_s is the stator inductance, R_r is the rotor resistance, L_r is the rotor inductance, L_m is the mutual inductance, $\sigma = 1 - L_m^2/(L_r L_s)$ represents the total leakage factor, $\lambda_{s\alpha\beta}$ is the stator flux, and $\lambda_{r\alpha\beta}$ is the rotor flux in the stationary reference frame. The superscript "s" denotes the stationary reference frame.

The proposed block diagram of a stand-alone DFIG with the stator voltage compensation method is presented in Fig. 3. The magnitude of the stator voltage is directly controlled with a given specific command value v_s^* by adding an external voltage control loop. The specific magnitude of the stator voltage is obtained from the positive sequence components of the measured voltage signals and is expressed by:

$$v_s = \sqrt{v_{sd+}^{+2} + v_{sq+}^{+2}}. \tag{9}$$

The stator voltage control loop is implemented using a PI controller to regulate the stator voltages in a stable manner. This control loop mainly aims to reject voltage variations due to the effect of electric loads or speed changes.

2.2 Calculation of Reference $\alpha\beta$ Rotor Currents

The proposed PR controller is used to precisely track the reference rotor currents that are determined based on four rotor current components, i.e., i_{rd+}^{+*}, i_{rq+}^{+*}, i_{rd-}^{-*}, and i_{rq-}^{-*}. The desired control target is to eliminate the negative sequence components, i.e., v_{sd-}^{-} and v_{sq-}^{-}, in generated stator voltages. Therefore, four controllable rotor current components was implemented in the RSC to effectively satisfy the system operation. As shown in Fig. 3, the reference negative sequence components of rotor currents, i.e., i_{rd-}^{-*} and i_{rq-}^{-*}, are the outputs of the two PI controllers. In this work, these controllers were used to drive the negative sequence components of the stator voltage to zero in the negative rotating reference frame. To obtain v_{sd-}^{-} and v_{sq-}^{-}, two notch filters were used to extract the values from their respective components in the negative rotating reference frame.

To apply the PR current controller in the stationary reference frame, four previously determined reference rotor current values were transformed into coordinates $\alpha_s\beta_s$ using the synchronous angles θ_s. This was calculated using:

$$i_{r\alpha\beta}^{s*} = i_{r\alpha\beta+}^{s*} + i_{r\alpha\beta-}^{s*} = i_{rdq+}^{+*} e^{j\theta_s} + i_{rdq-}^{-*} e^{-j\theta_s} \tag{10}$$

For comparison with the performance of the proposed current controller, a conventional PI regulator was implemented in the positive synchronous reference frame. In this frame, the reference rotor currents were determined as:

$$i_{rdq}^{+*} = i_{rdq+}^{+*} + i_{rdq-}^{-*} e^{-j2\theta_s} \tag{11}$$

These reference rotor currents consisted of both dc and ac components at twice the synchronous frequency. Even using PI regulator in the synchronous rotating frame, satisfactory control performance still cannot be achieved because of the finite gain when regulating the ac components. Therefore, the proposed PR current controller in stator stationary frame is the superior approach in accurately and effectively regulating rotor current.

3. The Proposed PR Current Controller

3.1 Advantageous Characteristics of the PR Regulator

Upon obtaining the reference rotor currents in the stationary reference frame in (10), these were controlled to achieve the control target, i.e., eliminating stator voltage imbalance. The use of a notch filter for decomposing the positive and negative sequence components of the control variables causes more time delay due to computational

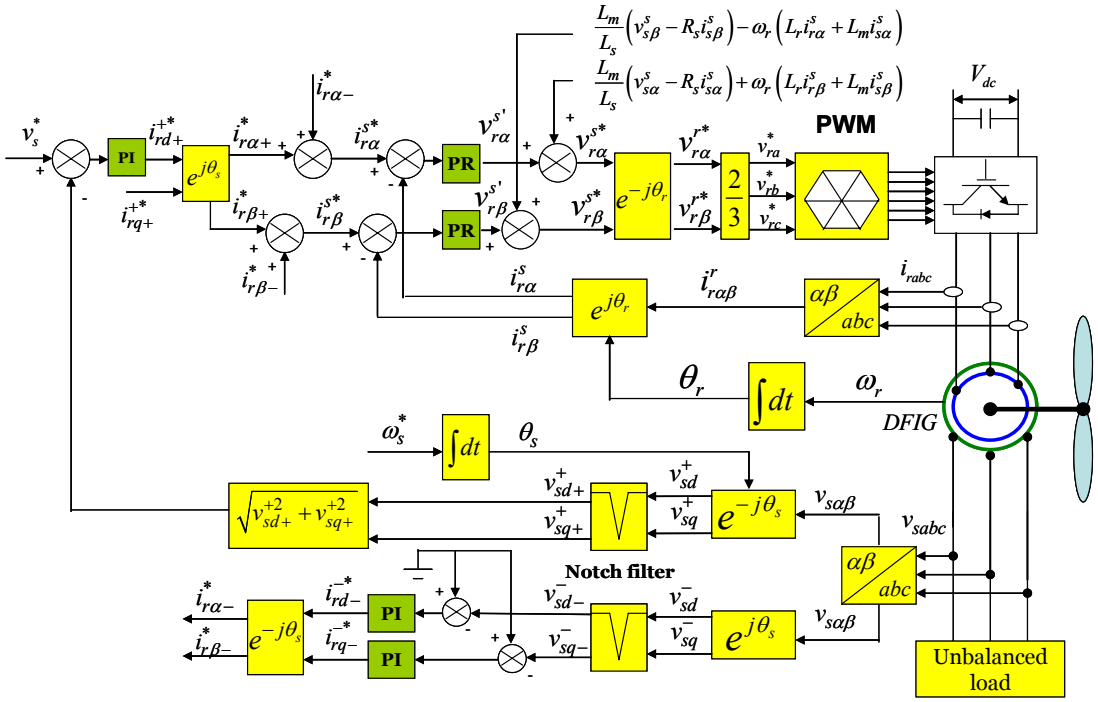

Fig. 3. Proposed current control scheme for the RSC of a DFIG under an unbalanced load using a PR controller in the stationary reference frame

complexity, thereby degrading the control system. The decomposition process of measured rotor currents can be practically implemented by digital notch or low-pass filters. Under an unbalanced load condition, the control system for a DFIG must be controlled precisely during the transient process and in the steady-state. Decomposing control signals in inner current control loops significantly degrades system stability and overall efficiency.

The PR controller applied to the RSC of a DFIG was employed in this study to improve the accuracy of the control system. One of the most important features of the resonant controller is that it is capable of sufficiently tracking the AC reference current, and therefore, can eliminate steady-state control variable errors at the chosen (resonant) frequencies. The s-domain open-loop transfer function of the proposed PR current controller is defined as:

$$G_o(s) = K_p + \frac{K_r s}{s^2 + \omega_s^2}, \tag{12}$$

where K_p is the proportional gain that has the same function in the PI controller; K_r denotes the resonant gain, which provides the infinite gain for AC component tracking; and ω_s is the resonant frequency equal to the synchronous frequency of the stator voltage outputs.

Fig. 4 describes the magnitude and phase characteristics of the open loop transfer functions for both the PI and PR controllers with respect to different values of the resonant gain K_r. The large gain produced at the resonant frequency

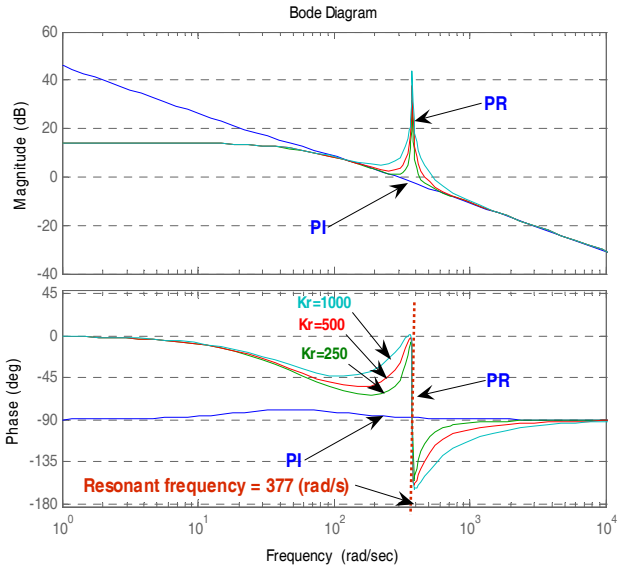

Fig. 4. Bode diagrams of open loop PI and PR controllers.

ensures that the steady-state errors in the rotor currents can be completely eliminated. Furthermore, the selection of resonant gain values determines the cross-over frequency and dynamic response of the control system. As illustrated in Fig. 4, a low K_r gives a very narrow bandwidth, whereas a high K_r leads to larger bandwidth. Fig. 5 shows the bode-diagram of the closed-loop transfer functions of the PR current controller compared with the conventional PI controller. The gains used in both bode-

diagrams were determined based on the Naslin polynomial technique, which was introduced in [13]. As shown in Fig. 5, the proposed controller with the resonant controller provided more accurate control with the characteristic of unity gain (0 dB) and minimum phase error at the resonant frequency, i.e., the synchronous frequency $f_s = 60\,Hz$. In contrast, the control bandwidth of the PI controller is not sufficient to regulate at the same resonant frequency.

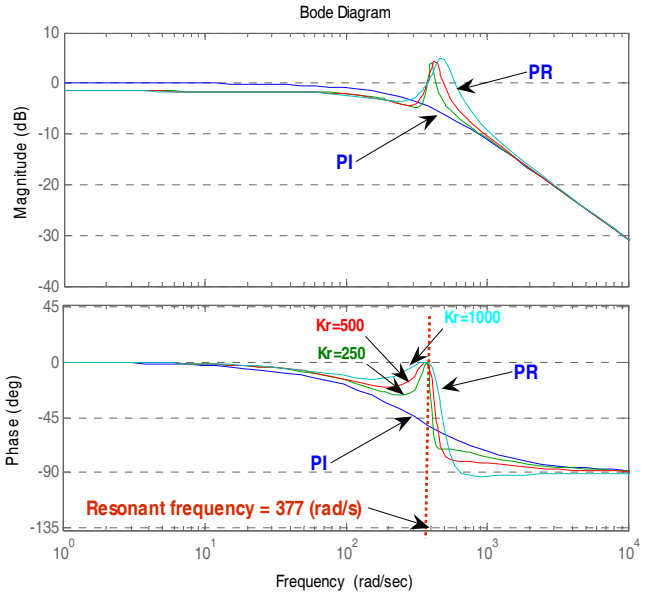

Fig. 5. Bode diagrams of closed-loop PI and PR controllers.

3.2 Stability Analysis

A closed-loop current control scheme in the RSC is described in Fig. 6. An analytical investigation regarding its frequency response when operating in a closed-loop system was conducted in order to determine if the proposed controller could achieve zero steady-state control error. The closed-loop transfer function of the control scheme is given by:

$$G_c(s) = \frac{i^s_{r\alpha\beta}}{i^{s*}_{r\alpha\beta}} = \frac{G_o(s)}{(\sigma L_r s + R_r) + G_o(s)} = \frac{K_p(s^2+\omega_s^2) + K_i s}{(s^2+\omega_s^2)(\sigma L_r s + R_s) + K_p(s^2+\omega_s^2) + K_i s} \quad (13)$$

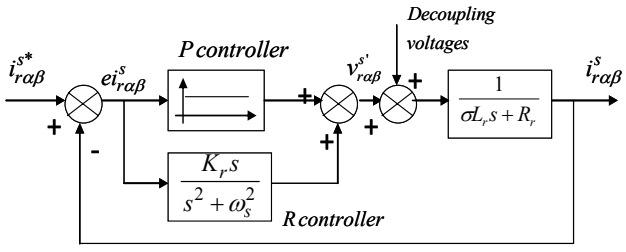

Fig. 6. The proposed PR current controller

Substituting $s = \pm j\omega_s$ into (12), the frequency response of the closed-loop transfer function at the $\pm\omega_s$ synchronous frequency is equal to 1, as computed in (14). This indicates that good control system performance can be obtained with unity gains and zero phases.

$$G_c(s)\big|_{s=\pm j\omega_s} = 1,\ \angle G_c(s)\big|_{s=\pm j\omega_s} = 0 \quad (14)$$

Based on the results, the proposed controller can precisely track the current control variables with zero steady-state error at a specific resonant frequency $\pm\omega_s$, regardless of the effect of the generator parameters R_r and σL_r.

3.3 Implementation of the Control Scheme

The errors between the reference and measured rotor currents are the inputs of the PR controller. The required control voltages that have been applied to the converters are the outputs of the proposed current controller. The output rotor voltages are determined by:

$$v^{s'}_{r\alpha\beta} = G_o(s)\left(i^{s*}_{r\alpha\beta} - i^s_{r\alpha\beta}\right) = \left(K_p + \frac{K_r s}{s^2+\omega_s^2}\right)\left(i^{s*}_{r\alpha\beta} - i^s_{r\alpha\beta}\right). \quad (15)$$

To improve decoupling between the $\alpha\beta$ components of the rotor currents, the decoupling voltage components shown in Fig. 3 were added to (15), after which the reference voltages for $\alpha\beta$ components became (16) and (17), respectively. These parameters compensate for unknown quantities equivalent to disturbances caused by the rotor back-electromagnetic force (EMF).

$$v^{s*}_{r\alpha} = v^{s'}_{r\alpha} + \frac{L_m}{L_s}\left(v^s_{s\alpha} - R_s i^s_{s\alpha}\right) + \omega_r\left(L_r i^s_{r\beta} + L_m i^s_{s\beta}\right) \quad (16)$$

$$v^{s*}_{r\beta} = v^{s'}_{r\beta} + \frac{L_m}{L_s}\left(v^s_{s\beta} - R_s i^s_{s\beta}\right) - \omega_r\left(L_r i^s_{r\alpha} + L_m i^s_{s\alpha}\right) \quad (17)$$

The modulation index of the doubly-fed induction machine must be performed in a rotor-oriented frame; thus, the outputs of the rotor current controller have to be transformed from the stator stationary reference frame to the rotor reference frame, which is identified as:

$$v^{r*}_{r\alpha\beta} = v^{s*}_{r\alpha\beta}\, e^{-j\theta_r}. \quad (18)$$

4. Simulations and Experimental Results

Simulations and experiments were carried out to verify the dynamic behavior of the proposed control method. The

simulation process was performed using PSIM software. The experimental platform was set up in a laboratory so as to implement the DFIG system and verify the proposed control scheme. Fig. 7 shows the experimental setup. The system consisted of a 2.2 kW DFIG, rotated by a DC motor, which was emulated as a prime mover with torque and speed control. The RSC was fed by an insulated-gate-bipolar-transistor (IGBT)-based PWM inverter with a switching frequency of 10 kHz. The system was developed with a high performance DSP TMS320F28335 (Texas Instruments). The generator was operated under unbalanced loads to test the dynamic performance of the proposed controller. The line to the neutral stator voltage was controlled at about 145 V. The unbalanced loads for the tests were one phase imbalance $30\Omega, 50\Omega, 50\Omega$ for each phase. Each load subset was connected to one of the three-phase stator terminals, namely, A, B, and C.

The dynamic performances of the proposed PR current controller in the RSC were investigated with the constant rotor speed at 1100 rpm. Fig. 8 shows the results of rotor current waveforms in the stationary and rotor reference frames. As previously analyzed, the purpose of the control scheme is to eliminate the negative sequence components included in stator voltages by controlling the rotor current in stationary reference frame. In this work, the stator voltages were well-compensated (Fig. 8), achieving the unbalance condition in a stable manner. Likewise, very good agreement was observed between the simulated and experimental results with the same conditions.

As for the steady-state performance of the rotor currents under the unbalanced operation system, the actual rotor currents in the stationary reference frame, i.e., $i^s_{r\alpha\beta}$ were well tracked according to the reference values to obtain the balanced stator voltages (Fig. 9). In the stationary reference frame, the rotor currents, $i^s_{r\alpha\beta}$, became sinusoidal waveforms with the synchronous frequency of the stator output. However, these currents were unbalanced due to the negative sequence components. Meanwhile, the measured rotor currents $i^r_{r\alpha\beta}$ in the rotor reference frame were far from the sinusoidal waveforms to compensate for the stator voltage imbalance. Therefore, the ripples occurred in the rotor

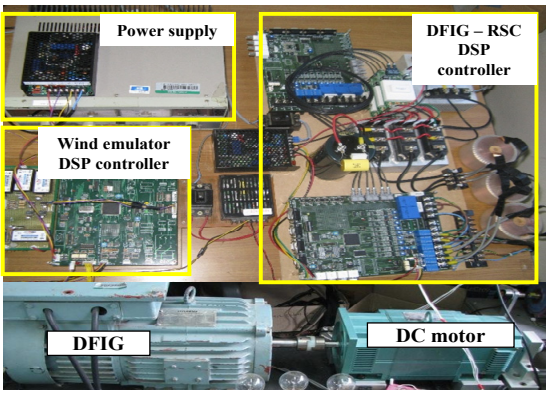

Fig. 7. Configuration of experimental setup.

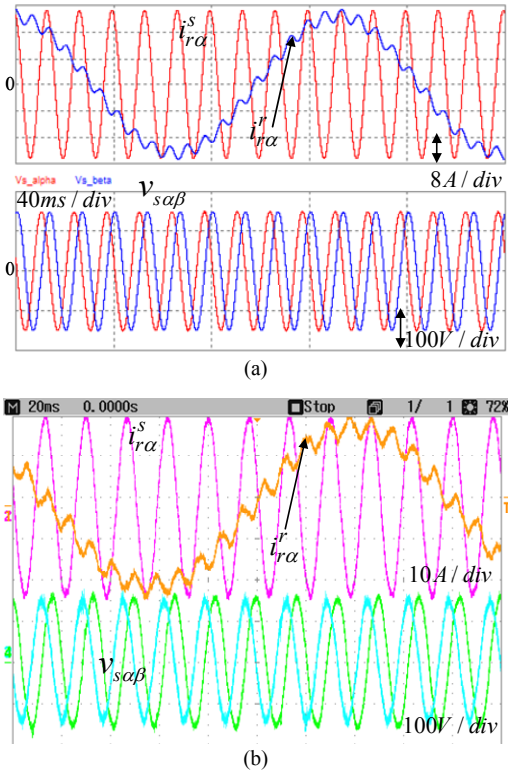

Fig. 8. Performance of the rotor currents and compensated stator voltages; (a) simulated results (b) experimental results.

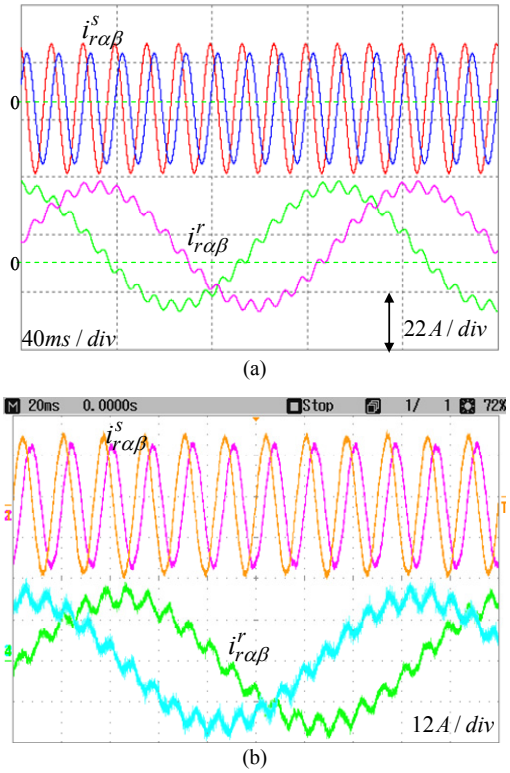

Fig. 9. Performance of the rotor currents in the $\alpha_s\beta_s$ and $\alpha_r\beta_r$ reference frames; (a) simulated results (b) experimental results.

current waveform (Fig. 9). The tested results can be obtained with simulations and experimental implementation.

Experimental tests were also performed under rotor speed variations to test the effectiveness and robustness of the proposed controller. The rotor speed varied from 1100-1300 rpm, i.e., from sub-synchronous to super-synchronous speed. The rotor currents during speed changes were effectively regulated (Fig. 10). The rotor current frequency decreased to almost zero at synchronous point of 1200 rpm. After that, it increased due to variations of the rotor slip so that the constant stator frequency can be kept. Based on the analysis, it can be concluded that the proposed control strategy can be applied in variable-speed wind turbine applications.

To prove good performance of the proposed current controller, a conventional PI regulator is used in the synchronous rotating frame for comparison. Fig. 11 shows experimental results of the d-axis rotor current and the stator output voltage with the use of PI regulator. The PI controller in the synchronous frame did not obtain satisfactory performance when regulating the rotor current including the ac component, described in (11) (Fig. 11). To easily compare with the proposed current controller, the rotor currents controlled in the synchronous rotating frame with the PI regulator are transformed to the stator stationary reference frame. Comparative results between the two methods are shown in Fig. 12, which shows that PR control strategy gave more adequate and accurate control than that obtained

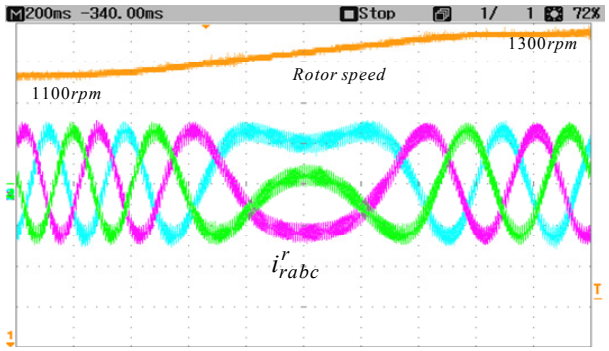

Fig. 10. Dynamic response of rotor currents through the synchronous speed.

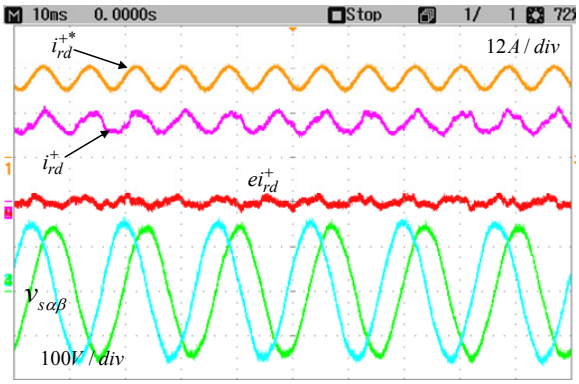

Fig. 11. The rotor current response in the synchronous rotating frame with the use of the conventional PI controller and the compensated stator voltage.

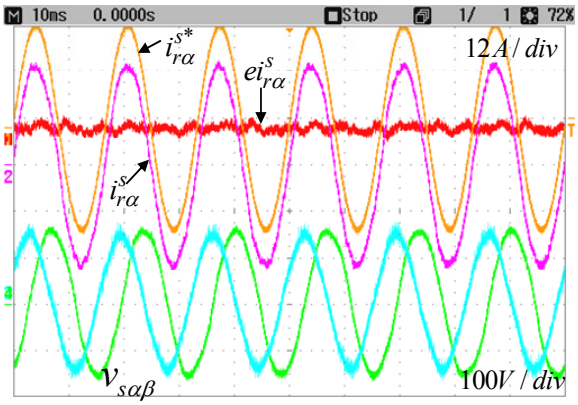

(a) PR controller

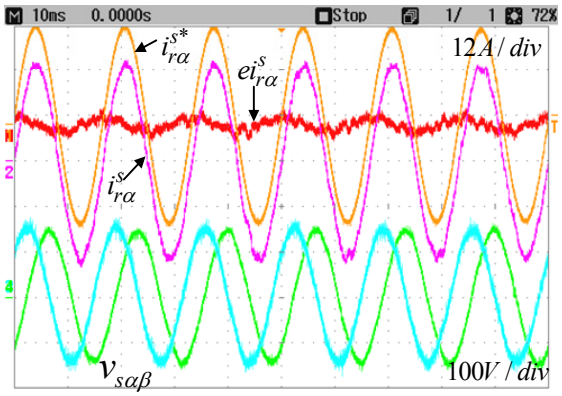

(b) PI controller

Fig. 12. Comparative results in terms of control accuracy and steady state performance of the rotor current and corresponding compensated stator voltages

with the PI controller due to its limited control bandwidth when regulating at the synchronous (resonant) frequency. Taking into account the steady state error of rotor current in the stationary reference frame, precise current control can be achieved with the PR controller. As a result, the unbalanced stator voltages were well compensated. In contrast, the control scheme with the traditional PI controller gave unsatisfactory results in terms of control correctness and steady state performance under the unbalanced DFIG system.

5. Conclusions

An enhanced control scheme using the PR controller for unbalanced stand-alone DFIG systems was investigated in this paper. The proposed current controller was implemented in the stator stationary reference frame for controlling positive and negative sequence components without the sequential decomposition of the measured rotor currents. Consequently, the desired control target, i.e., eliminating the negative sequence components in unbalanced stator voltages, was well achieved with the proposed control method. Comparative results between the proposed and the conventional PI controllers indicated the ability of the former to perform a more precise and adequate control of

the proposed control strategy. The feasibility and effectiveness of the proposed method were proven through theoretical analysis, simulations, and experimental results.

Acknowledgements

This work was supported by the Human Resources Development of the Korea Institute of Energy Technology Evaluation and Planning(KETEP) grant funded by the Korea government Ministry of Knowledge Economy (No. 2007-P-EP-HM-E-04-0000).

References

[1] Daniel G. Forchetti, Guillermo O. Garcia, and Maria Ines Valla, "Adaptive observer for sensorless control of stand-alone doubly fed induction generator," *IEEE Transactions on Industrial Electronics*, Vol. 56, No. 10, pp. 4174-4180, Oct. 2009.

[2] Pena, J. C. Clare, and G. M. Asher, "A doubly fed induction generator using back-to-back PWM converters supplying an isolated load from a variable speed wind turbine," *IEE Proc. Electric Power Applications*., Vol. 143, No. 5, pp. 380-387, 1996.

[3] S. Muller, M. Deicke, R.W, and De Doncker, "Doubly fed induction generator system for wind turbines," *IEEE Industry Application Magazine*, Vol. 8, No. 3, pp. 26-33, May. 2002.

[4] Arantxa Tapia, Gerardo Tapia, J. Xabier Ostolaza, and Jose Ramon Saenz, "Modeling and control of a wind turbine driven doubly fed induction generator," *IEEE Transactions on Energy Conversion*, Vol. 18, No. 2, pp. 194-204, June. 2003.

[5] Ted K. A. Brekken and Ned Mohan, "Control of a doubly fed induction wind generator under unbalanced grid voltage conditions," *IEEE Transactions on Energy Conversion*, Vol. 22, No. 1 pp. 129-135, Mar. 2007.

[6] Lie Xu and Yi Wang, "Dynamic modeling and control of DFIG-based wind turbine under unbalanced network conditions," *IEEE Transactions on Power Systems*, Vol. 22, No. 1 pp. 314-323, Feb. 2007.

[7] Lie Xu, "Coordinated control of DFIG's rotor and grid side converters during network unbalance," *IEEE Transactions on Power Electronics*, Vol. 23, No. 3 pp. 1041-1049, May 2008.

[8] Lie Xu, "Enhanced control and operation of DFIG-based wind farms during network unbalance," *IEEE Transactions on Energy Conversion*, Vol. 23, No. 4 pp. 1073-1081, Dec. 2008.

[9] Pena, R., Cardenas, R., Escobar, E. Clare, J., and Wheeler, P., "Control System for Unbalanced Operation of Stand-Alone Doubly Fed Induction Generators," *Energy Conversion, IEEE Transactions on*, Vol. 22, No. 2, pp. 544-545, June 2007.

[10] Pena, R., Cardenas, R., Escobar, E., Clare, J., and Wheeler, P., "Control strategy for a doubly fed induction generator feeding an unbalanced grid or stand-alone load," *Electric Power Systems Research*, July. 2008.

[11] R. Teodorescu, et al., "Proportional-resonant controllers and filters for grid-connected voltage source converters," *Electric Power Application*, IEE Proceedings, Vol. 153, No. 5 pp. 750-762, Sep. 2006.

[12] Marco Liserre, Remus Teodorescu, and Frede Blaabjerg, "Multiple harmonics control for three-phase grid converter systems with the use of PI-RES current controller in a rotating frame," *IEEE Transactions on Power Electronics*, Vol. 21, No. 3 pp. 836-841, May 2006.

[13] Marian P. Kazmierkowski, R. Krishnan, and F. Blaabjerg, "Control in Power Electronics: selected problems", Academic Press, 2002.

Van-Tung Phan was born in Binh Dinh province, Vietnam, in 1982. He received his B.S. degree in Electrical Engineering from the University of Technology, Ho Chi Minh City, Vietnam, in 2005. Since Sept. 2005, he has been with the Department of Electrical Engineering, University of Ulsan, Korea, where he has been undertaking graduate study under the Master's and Doctoral Degree programs. His research interests include power electronics, applications of DFIG and PMSG, and advanced control techniques applied to wind power systems.

Hong-Hee Lee (M'96) is a professor at the School of Electrical Engineering, University of Ulsan, Ulsan, Korea. He is also the Director of Network-based Research Center (NARC). He received his B.S., M.S., and Ph.D. degrees in Electrical Engineering from Seoul National University, Seoul, Korea, in 1980, 1982 and 1990, respectively. He is also a member of Institute of Electrical and Electronics Engineers (IEEE), Korean Institute of Power Electronics (KIPE), Korean Institute of Electrical Engineers (KIEE), and Institute of Control, Automation, and Systems Engineers (ICASE). His current research interests include power electronics, network-based motor control, and control network.